

A low-cost podoscope for extracting morphological features of the foot

Ruba Musaid¹, Aseel Ghazwan¹, Waleed A. Al-Saadon²

Biomedical Engineering Department, Al-Nahrain University, Baghdad, Iraq¹
Consultant Orthopedic Surgeon, Medical City teaching complex, Baghdad, Iraq²

ABSTRACT

Foot morphology evaluation techniques are commonly used to evaluate foot abnormalities. The foot is essential for keeping the biomechanical performance of the lower extremities. It is responsible for the support of body balance and stability during gait. For the qualitative examination of foot morphology, many podoscopes have been designed. However, these podoscopes are mainly expensive, complex to operate, and have low accessibility. As a consequence the goal of this research was to create a simple, low-cost podoscope to assess the plantar footprint. In addition to providing a visual representation of the supporting regions. The proposed system enables accurate estimation of clinical indexes of foot deformities. With bare feet, bipedal support, and orthostatic posture, the participant was placed on the podoscope. Doom camera was used to capture the image of the plantar of the foot, and the data was sent to a computer via LAN connection. Based on image processing techniques, the proposed podoscope can automatically estimate the Arch Index, the Chippaux-Smirak Index, the Staheli Index, and Wejsflog's index. Ten samples were tested by the proposed podoscope, and the calculated parameters defining foot deformities are presented. The proposed podoscope appears to have the advantages of simplicity, being portable, inexpensive enabling rapid and precise footprint assessment with correct diagnoses, as well as a record for future assessments, and being economically viable in countries with people having low socio-economic status.

Keywords: Podoscope, Arch Index, Chippaux-Smirak Index, Staheli Index, Wejsflog's index.

Corresponding Author:

Ruba Musaid
Biomedical Engineering Department,
Al-Nahrain University. Baghdad, Iraq.
E-mail: ruba92haydr@gmail.com

1. Introduction

The human body's foot is a complicated bone structure kept together by tendons and muscles. This not only maintains the weight of the upper body but also cushions shock during motion [1] and reduces back pain [2]. The tarsal and metatarsal bones create foot arches, which are supported by tendons and ligaments. Transverse arches, medial longitudinal arches (MLA), and lateral longitudinal arches (LLA) are the structural classifications of foot arches. Foot deformity development differs by the cause of degenerative alterations in the osteoarticular system, which affect statically foot performance. One of the many pathology responsible for the emergence of joints damage is, biomechanical factors as pressure, slip resistance, synovial viscosity, and changes in the friction coefficient are often given special consideration. Alteration in the biomechanics of the locomotor system results in joint restricted mobility throughout time, pain disorders with varied clinical symptoms and development dynamics, limb orientation deformations, joint contractures, and a distorted inefficient gait pattern [3]. Rheumatoid arthritis (RA) and Osteoarthritis (OA) are the most often described pathological conditions that lead to the progress of foot deformities [3, 4]. Normal changes in the lower limb's major joints, for example, the knee and hip joints, have an impact on the biomechanics of the whole kinematic chain. As a natural response to the damaging process that affects joint surfaces and periarticular tissues, the body experiences elevated muscular tension, as a result of the lower limb's overload bio kinematic chain. Incorrect limb positioning causes deformations that, if untreated, become permanent [5].

Different methodologies, including radiographs, ultrasound, and footprint measurements, have been introduced to classify foot deformities as cavus, planus, or normal.

There are various difficulties in radiological examination, considering the complexity of calculating the angles defining foot type, variations in image quality caused by varied radiologic technician skills, interobserver or intraobserver error, as well as exposure to radiation [6-8].

In addition to that, real-time ultrasound imaging is one of the objective technologies used to examine plantar fascia [9]. Images of the morphology for foot muscles and thus the foot fascia with cross-sectional areas (CSAs) were acquired using B-mode ultrasound [10]. Ultrasonic procedures, on the other hand, must be carried out by a skilled specialist.

The footprint is an alternate method of assessing foot morphology. A big thin sponge (bigger than the area of a foot) was put on a dish, then ink diluted with water was sprayed over it. To obtain footprint, the foot was rapidly put on a sheet of paper [11, 12]. The accuracy of this approach is poor, which might be related to a number of limitations, such as inadequate adhesion to that of the plantar surface, insufficient or high ink penetration in the paper, error while measuring values from ink footprints. Furthermore, when more than three or four trial measurements were taken, the accuracy of the ink footprint was lost. It makes the footprint darker, making it harder to measure and imprint newer areas with sharp edges [13].

Earlier research was largely concerned with foot problems and abnormalities. The increased interest in foot pressure led to the development of a novel measurement of plantar foot pressure. Various foot pressure devices (plantar platform system and in-shoe system) have been developed, [14, 15]. The plantar platform technique has the disadvantage of requiring patient familiarization to guarantee a natural gait and for an accurate reading, the foot must make contact with the centre of the sensing region [16]. The in-shoe technique, sensors must be correctly fixed to avoid slippage and give accurate information [16]. Regardless of the type of device, whether it is an in-shoe system or a plantar platform system, it requires accurate software and the technical expertise of the user, making it quite expensive.

Among the several techniques used to assess foot deformities, the optical podoscope is one of the most basic for a static assessment [17]. The podoscope's main concept is based on the usage of a transparent surface (generally glass) to capture the picture with the aid of a camera, where appropriate lighting is necessary. Although pricey, high-quality podoscopes are in demand. As a result, much research has concentrated on the design and fabrication of low-cost podoscopes with accurate results.

Different podoscopes have been introduced and are characterized according to the material of the supporting structure, i.e., a metal [18-20] or wood [13, 21, 22], the translucent surface, i.e., transparent glass [13, 23, 24] or plastic back-illuminated top [25]. Some have a mirror to reflect the image to the camera [21]. A camera [19, 21, 24] or a scanner [13, 23] was used to capture the image. The captured image is displayed by computer [13, 21, 22] or mobile [19] through the Internet [19] or USB cable [18, 24]. Using AutoCAD software, the image calibration approach was used to measure the parameters [13, 26] or matlab [24] or OpenCV library [18].

2. Materials and methods

Foot arch integrity is assessed using standard parameters (Arch index (AI), Chippaux-Smirak index (CSI), and Staheli index (SI)). An individual's arch index (AI) was determined by dividing the area of the centre third of the footprint divided by its total area, excluding the toes. The length of the foot (excluding the toes) is split into three equal thirds to identify the area of forefoot (A), the area of midfoot (B), and area of the heel (C). The arch index is then determined by dividing the area of the midfoot (B) by the total footprint area [27].

$$AI = \frac{B}{(A+B+C)} \quad (1)$$

The index's normal values varied from 0.21 to 0.26. Values larger than 0.26 indicate that the feet are longitudinally flat [28].

Chippaux-Smirak index (CSI): can be expressed as the ratio of the foot's width at the level of the narrowest point on the foot arch to the that at the metatarsals [29].

$$CSI = \frac{B}{A} \times 100\% \quad (2)$$

The normal foot category's CSI range was $0.25 \leq CSI < 0.45$. For the flatfoot, $CSI \geq 0.45$. For the cavus foot, it was $0 < CSI < 0.25$ and for the extreme cavus, it was $CSI = 0$ [20, 30].

The Staheli arch index (SI): can be described as the ratio of the foot's width at the level of the narrowest point on the foot arch to the maximum width at the heel region [29].

$$SI = \frac{B}{C} \times 100\% \quad (3)$$

This technique considers ratios (0.50 _ 0.70) to be normal, whereas ratios over 0.70 to be pes planus [31]

Wejsflog's index: which is the foot length to foot width ratio, is used to diagnose transverse flatfoot[32-34]. The value of this index remains between 2 and 3, and transverse flatfoot may be identified when it is closer to 2, while it is normal when it is closer to 3 [32-34]. it is recommended that assessment of foot posture.

All parameters were described in (Figure. 1)

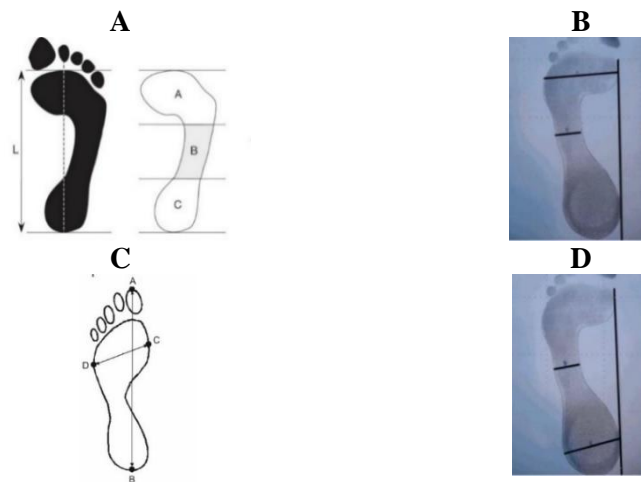


Figure 1. Footprint with a reference line to calculate (A) arch index [21]; (B) Chippaux smirak index [23]; (C) Wejsflog's index [7]; (D) Staheli index [23]

Accordingly, the goal of this project was to use a simple, low price, convenient with available component system for assessing foot deformities can be a good tool for daily evaluation by measuring several parameters to obtain accurate results regarding morphology of foot. The suggested system's design is produced at the lowest feasible cost using affordable resources. The following are the components of the device: For frame, the iron material construction was employed to create a stable support for high weights. (135kg) with dimensions (22 Height, 39 Width, 44 Length) centimeters, as shown in Figure 1(A). Iron sheets around the frame were utilized to form and protect the device's camera. The iron frame was painted white and nickel clamps were used to hold the portable podoscope, as shown in Figure 2(B) a door on the device's side was built to allow for camera repair as required.



Figure 1. (A) Iron frame; (B) Final shape of the podoscope

The podoscope structure must be able to handle a maximum weight of about 135 kg. As a result, Tempered glasses with a thickness of 12 millimeters should be used. The glass arrangement consists of two layers: The top layer is tempered glass, which allows light from the LED to be dispersed during its surface to identify the footprint. A lower layer of gray glass filters out external illumination sources. Grey glass with a transmission percentage of 14% is employed in this research.

That is critical to adjust the white LED lights all around glass since moving the light source produces an insufficient image for handling. The LED requirements that were utilised have a 9-10W, 5730 k, 10 cm cut, 100 LED with 45-50 lumens/LED illumination system. Through the experience of these specifications of LED, good illumination and distribution through the glass were accomplished as shown in (Figure. 3).

A doom) digital video camera) type camera, (as shown in Figure 2) the camera is installed in the middle of a wooden base, was used to capture the image and connect it to the computer via a LAN cable, where the image was displayed using the VICON Motus Software (VMS) program with the specification:

Camera 5MP, Model number I505D, LENS 4mm, power 12V DC or 48V POE, Infrared waterproof, Latest DSP digital signal processing technology, Exclusive Korean latest program, Image stabilization technology.

Computer: Lenovo type with MATLAB code version 2022 has been installed. As a first stage, the entire subject's foot was sprayed with water and carefully dried with a towel. On the podoscopic instrument, each participant was asked to stand erect and face ahead; after a few attempts of getting to know the system, The camera's images were sent to the computer.

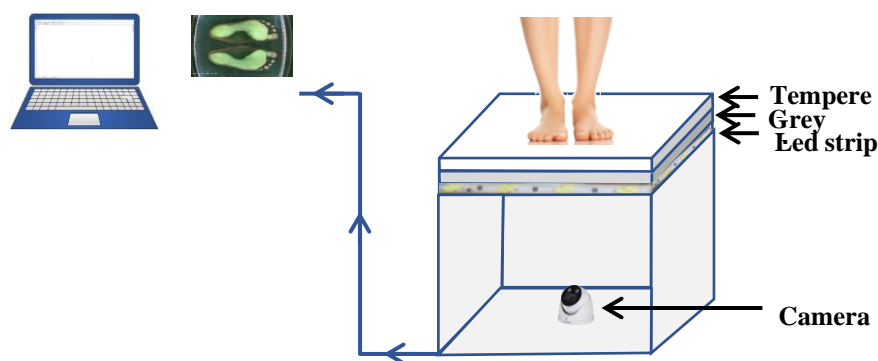


Figure 3. The components of the proposed podoscope structure

In the proposed approach, a tool has been created utilising free software for evaluating the footprint by getting the footprint profile and semiautomatically drawing reference points and lines to aid in the estimate of clinical indices.

The footprint image was captured with a doom-type camera, where images are in JPG format with pixel dimensions and RGB colour space. The images are sent to the computer via a LAN cable and displayed using the VICON Motus Software (VMS) program all steps of process was shown in Figure 4.

The footprints were easily visible as a result, it extracts and collects the parameters using the Matlab interface. The image has a green tone in the footprint areas and a black tonality on the outside, thereby reaching simplicity in digital image processing.

Once the image is introduced, pre-processing steps are made. Firstly, the image was cut into two parts, each part containing right or left foot. This was done manually before entering the image into the MATLAB code for image processing. The algorithm of MATLAB starts by importing the image with JPG extension. Then, the image is cropped, where cropping part of the image instead of processing the whole image makes the process easier and simpler for the software to handle.

Image processing procedures include filtering, contrast adjustment, edge recognition, and more. The final image will differ according to the system designer and excellent image.

Calculating the threshold and converting the grayscale image to binary in order to reduce the intraclass variation of the black and white pixels. Then this threshold converts the image to black and white. Finally, an applied Bwareaopen filter to remove the small pixels or objects from the binary images is obtain where bwareaopen (bw, P) removes all connected components (objects) that have fewer than P (maximum number of pixels in object) pixels from the binary image BW (binary image), producing another binary image, BW2. This operation

is known as an area opening. For further enhancement of the image, a median filter was used to eliminate the noise from the image without reducing the accuracy [35].

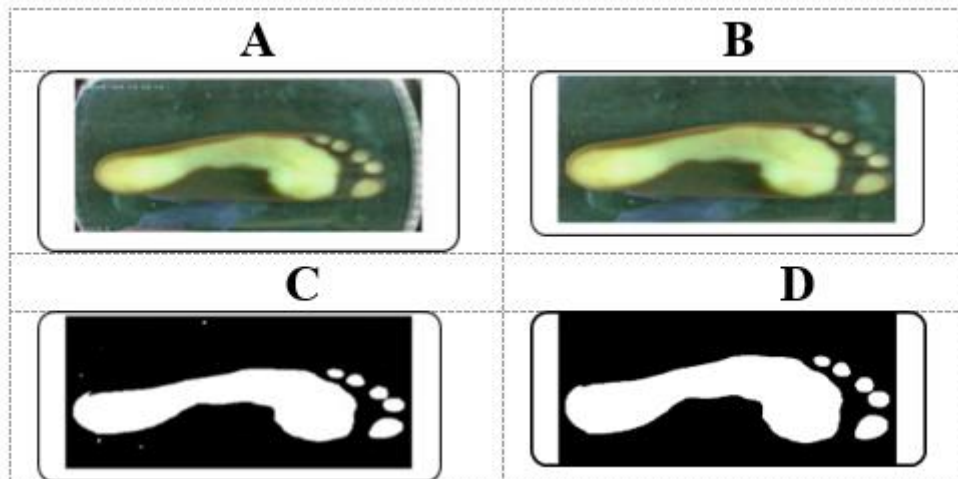
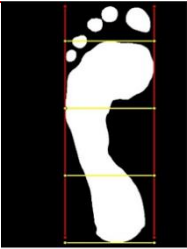


Figure 4. Image formatting: (A) reading the image, (B) cropping, (C) converting to binary, (D) filtering

Parameters were calculated after formatting the image and removing impurities, as summarized in Table 1.

Table 1 Steps for calculating morphological parameters

NO.	PARAMETER	IMAGE	DESCRIPTION
1	Arch index		Image after preprocessing (Convert Image to Binary & apply filters)
			Draw two lines that is parallel to foot (specify the left and right edges)
			Divide the palm into three equal regions. The white area was calculated for each region Arch index was calculated as eq(1).
2	Chippaux-Smirak index		The biggest width was Calculated in the white area (a) And the lowest width in white area (b) eq(2)was applied

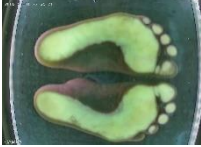
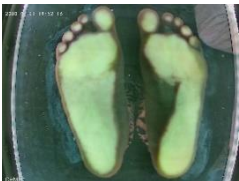
NO.	PARAMETER	IMAGE	DESCRIPTION
3	The Staheli arch index (SI)		The biggest width was Calculated in the white area (c) And the lowest width in white area(b) eq(3)was applied
4	Wejsflog's index		Length of foot was calculated, the width already was calculated previously Wejsflog's index was calculated as a ratio of length to width.

3. Results and discussion

Ten samples were tested by the proposed podoscope, and the calculated parameters defining foot deformities are presented in Table 2. Through the readings, the proposed podoscope have captured the foot deformities among participants which are illustrated with (*) sign. Samples (1-5), were approved by a consultant that they have normal foot. This is agreed with the output of the proposed podoscope, where the arch index and Wejsflog's index by CSI and SI. Samples (6, 7, 8), were approved by a consultant that they have cauves foot,(5,6)only the left is cauves the right normal, but the 7 both cauver, where the arch index and Wejsflog's index by CSI andSI. Samples (9, 10), were approved by a consultant that they have right flat with normal left foot, where the arch index and Wejsflog's index by CSI and SI.

Table 1. Measured parameters for assessing foot deformities

NO.	Feet print	Arch index		CSI Index		SI Index		Wejsflog's index			
		(AI)		RL	LL	RL	LL	RL	LL	RL	LL
		RL	LL	RL	LL	RL	LL	RL	LL	RL	LL
1		0.23	0.25	0.36	0.38	0.59	0.6	2.9	2.9		
2		0.25	0.22	0.41	0.35	0.64	0.52	2.8	2.79		
3		0.25	0.24	0.44	0.44	0.68	0.60	2.9	2.9		

NO.	Feet print	Arch index		CSI Index		SI Index		Wejsflog's index			
		(AI)		RL	LL	RL	LL	RL	LL	RL	LL
		RL	LL	RL	LL	RL	LL	RL	LL	RL	LL
4		0.26	0.24	0.45	0.36	0.67	0.45	2.7	2.5		
5		0.25	0.27	0.43	0.41	0.53	0.58	2.5	2.9		
6		0.21	0.19*	0.33	0.26*	0.47	0.39*	2.7	2.7		
7		0.22	0.18*	0.35	0.14*	0.50	0.21*	2.5	2.5		
8		0.15*	0.15*	13.5*	18.6*	19.4*	23.9*	2.6	2.9		
9		0.29*	0.28	0.47*	0.47	0.74*	0.71	3.04	2.62		
10		0.37*	0.25	0.73*	0.43	0.98*	0.62	2.7	3.1		

* represent that the reading is out of normal values; RL= right leg, LL=left leg. AI ranged (0.21-0.26) for normal foot, AI <0.28 for flat foot, AI >0.21 for high curved foot. $0.25 \leq \text{CSI} < 0.45$, for normal foot, $\text{CSI} \geq 0.45$ for

flatfoot, $0 < \text{CSI} < 0.25$ for high curved foot. SI ranged (0.50 - 0.70) for the flatfoot, $\text{SI} < 0.70$ for flatfoot, $\text{SI} > 0.50$ for high curved foot. Wejsflog's index ranged (2-3), close to 2 for flatfoot and close to 3 for normal foot.

The proposed podoscope succeeds in identifying foot morphology, automatically performing the appropriate analysis, transferring data to the computer, and storing and displaying foot abnormalities. This method removes error rates and speeds up the entire process. The proposed portable podoscope system described in this study has a weight capacity of roughly 135 kg. It can be carried by a single person to any location, allowing for free diagnosis and data collection in rural and underserved locations. The suggested podoscope was constructed in such a way that it does not require a technical expert to operate it. During the examination, the participant should stand on both feet on the platform and not move. Feet were carefully cleaned with water and wiped with a towel; this step is critical for increasing the clarity of the foot on the glass.

Other studies have employed two cameras, inside the system, [19] or one camera, outside the system, with a mirror at a certain angle to capture both feet [21]. To decrease the cost and components of the device, just one camera was used to capture the images in the suggested system; no mirror was employed, and the camera was positioned in the centre of the base. This, in turn, reduces errors caused by putting the camera out of the system, which requires calibration at each test, as well as the necessity to adjust a mirror to a certain angle in order to capture both feet. Different cameras have been tested, DOOM camera has shown to be the best choice; has highest range of view according to the dimension of the proposed system and low cost compared to the other cameras.

The external illumination is considered one of the main sources of noise. A study carried by [36] were used a dark fabric, which was placed to cover the platform to get rid of the illumination. However, using this method will not be able to visualize orthostatic posture for both feet during capturing. To solve this issue, a second layer of grey glass was added in the proposed system. This allows blocking of external illumination sources and acts as a filter to improve image quality. A suggested method was designed to transport data across a LAN line. In this regard, image processing technologies were used to assess and evaluate the footprint using Matlab. The tests' findings revealed that the recommended podoscope generated acceptable results with a reduced testing time, analyses the results, and retains data.

As for device's validation, a comparable sample was recorded on the BTS P-WALK baroresistive platform (BTS, Bioengineering, Italy), to assess AI based on foot pressure distribution in the forefoot, midfoot, and rearfoot, as shown in Figure 8_B. Prior to data collection the device was calibrated in accordance with the manufacturer's directions. Ink foot prints were used to evaluate the same participant's foot print, as shown in Figure 9.

AI was calculated for the same participant across the three methods to validate the suggested device's precision.

Table 2. Validation results of AI by applying three approaches

DEVICE	AI		STATE
	LF	RF	
Podoscope	0.22	0.25	Normal foot
BTS P-WALK	0.22	0.25	Normal foot
Foot print by ink	0.22	0.25	Normal foot

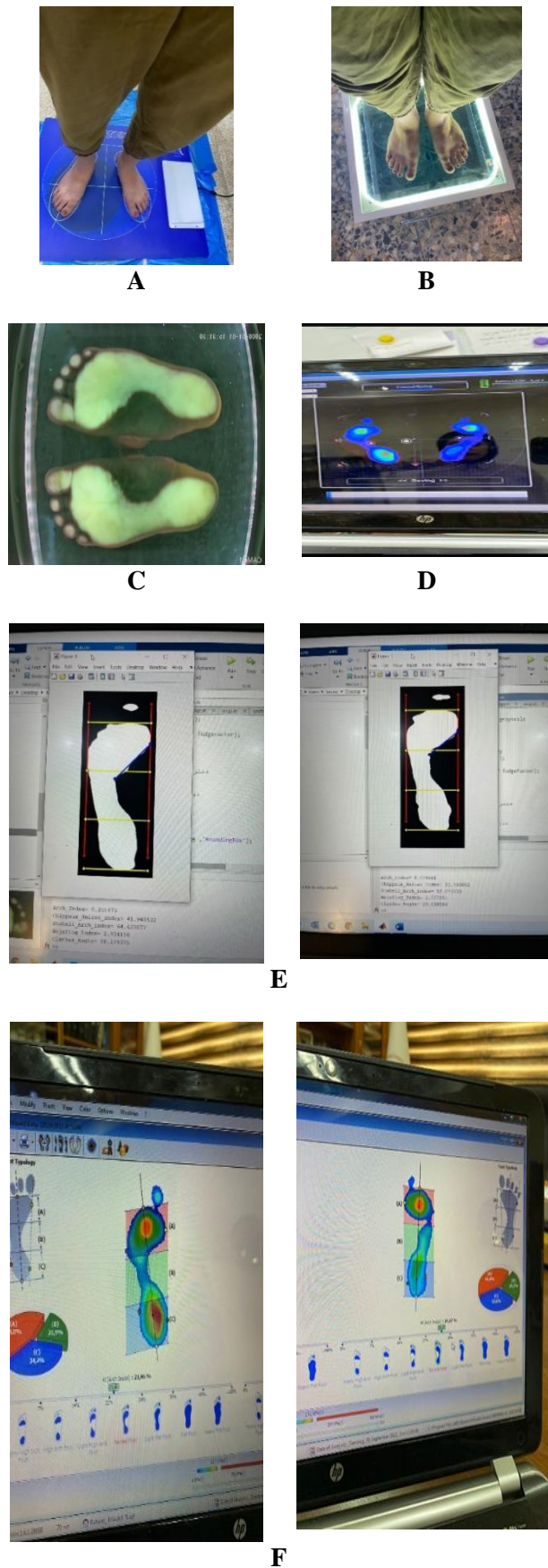


Figure 5. (A) The plantar platform footscan (BTS P-WALK) (B) proposed podoscope, (C) podoscope footprint (D) The plantar platform foot scan, (E) Right and left foot arch index (measured by the proposed podoscope), (F) Right and left arch index plantar platform footscan.



Figure 6. Ink footprint for validation arch index

4. Conclusion and future work

The device performs excellently in identifying foot's morphology, doing the necessary analysis automatically, transferring data to the computer, and storing and displaying the progression of foot abnormalities. This approach eliminates human mistakes and speeds up the procedure. This system's digital picture capture is paperless, meaning the patient's foot data can be saved for a very long time. Among the options for improving the suggested system, that can support more than 135kg weight and connect to the internet to send the data to anywhere.

Declaration of competing interest

The authors declare that they have no known financial or non-financial competing interests in any material discussed in this paper.

Funding information

No funding was received from any financial organization to conduct this research.

References

- [1] Y.-C. Lin, J. Y. Kwon, M. Ghorbanhoseini, and J. S. Wu, "The hindfoot arch: what role does the imager play?," *Radiologic Clinics*, vol. 54, no. 5, pp. 951-968, 2016.
- [2] K. Kitagawa, K. Yamamoto, and C. Wada, "Relationship between Foot Position and Lumbar Loads while Turning Patients on a Bed: An Investigation via Computational Simulation and Electromyography," *International Journal of Online & Biomedical Engineering*, vol. 17, no. 10, 2021.
- [3] C. L. Brockett and G. J. Chapman, "Biomechanics of the ankle," *Orthopaedics and trauma*, vol. 30, no. 3, pp. 232-238, 2016.
- [4] R. Barrois *et al.*, "An automated recording method in clinical consultation to rate the limp in lower limb osteoarthritis," *PLoS One*, vol. 11, no. 10, p. e0164975, 2016.
- [5] B. Yılmaz, S. Kesikburun, O. Köroğlu, E. Yaşar, A. S. Göktepe, and K. Yazıcıoğlu, "Effects of two different degrees of lateral-wedge insoles on unilateral lower extremity load-bearing line in patients with medial knee osteoarthritis," *Acta Orthopaedica et Traumatologica Turcica*, vol. 50, no. 4, pp. 405-408, 2016.
- [6] K. Iyengar *et al.*, "Calcaneal offset index to measure hindfoot alignment in pes planus," *Skeletal Radiology*, pp. 1-7, 2022.
- [7] Y.-C. Lin, J. N. Mhuirheartaigh, J. Lamb, J. W. Kung, C. M. Yablon, and J. S. Wu, "Imaging of adult flatfoot: correlation of radiographic measurements with MRI," *American Journal of Roentgenology*, vol. 204, no. 2, pp. 354-359, 2015.
- [8] K. Paliana, B. Jankharia, and P. Monoot, "Role of the weight-bearing cone-beam CT in evaluation of flatfoot deformity," *Indian Journal of Radiology and Imaging*, vol. 29, no. 04, pp. 364-371, 2019.
- [9] M. A. Mohseni-Bandpei, M. Nakhaee, M. E. Mousavi, A. Shakourirad, M. R. Safari, and R. V. Kashani, "Application of ultrasound in the assessment of plantar fascia in patients with plantar fasciitis: a systematic review," *Ultrasound in medicine & biology*, vol. 40, no. 8, pp. 1737-1754, 2014.

- [10] S. Taş, N. Ö. Ünlüer, and A. Çetin, "Thickness, cross-sectional area, and stiffness of intrinsic foot muscles affect performance in single-leg stance balance tests in healthy sedentary young females," *Journal of Biomechanics*, vol. 99, p. 109530, 2020.
- [11] A. Ramos, S. Fernandes, P. J. Panicker, and P. Krishnan, "Assessment of flat foot using plantar arch index in young adults," *Biomedicine*, vol. 41, no. 3, pp. 535-538, 2021.
- [12] M. Sawant Janhavi and B. Shinde Sandeep, "Effect of lower limb proximal to distal muscle imbalance correction on functional pes planus deformity in young adults."
- [13] K. Vijayakumar, R. Subramanian, S. Senthilkumar, and D. Dineshkumar, "An Analysis of Arches of Foot: A Comparison between Ink Foot Print Method and Custom Made Podoscope Device Method."
- [14] A. H. A. Razak, A. Zayegh, R. K. Begg, and Y. Wahab, "Foot plantar pressure measurement system: A review," *Sensors*, vol. 12, no. 7, pp. 9884-9912, 2012.
- [15] A. MN, "An Instrumented Insole System for Gait Monitoring and Analysis," *International Journal of Online Engineering*, vol. 10, no. 6, 2014.
- [16] B. MacWilliams and P. Armstrong, "Clinical applications of plantar pressure measurement in pediatric orthopedics," in *Pediatric gait: a new millennium in clinical care and motion analysis technology*, 2000: IEEE, pp. 143-150.
- [17] U. Kanatli, H. Yetkin, and E. Cila, "Footprint and radiographic analysis of the feet," *Journal of Pediatric Orthopaedics*, vol. 21, no. 2, pp. 225-228, 2001.
- [18] J. R. Maestre-Rendon *et al.*, "Low Computational-Cost Footprint Deformities Diagnosis Sensor through Angles, Dimensions Analysis and Image Processing Techniques," *Sensors*, vol. 17, no. 11, p. 2700, 2017. [Online]. Available: <https://www.mdpi.com/1424-8220/17/11/2700>.
- [19] T. Ahmadi and P. Cifuentes-Guerrero, "Remote Diagnosis of the Footprint Using a Portable-Podoscope System," *Annals of Medical and Health Sciences Research*, 2020.
- [20] R. M. Queen, N. A. Mall, W. M. Hardaker, and J. A. Nunley, "Describing the medial longitudinal arch using footprint indices and a clinical grading system," *Foot & ankle international*, vol. 28, no. 4, pp. 456-462, 2007.
- [21] H. Heravi, A. Ebrahimi, S. Nikzad, and E. Olyaei, "Low price foot pressure distribution screening technique: optical podoscope with accurate foot print segmentation using hidden Markov random field model," *Journal of Biomedical Physics & Engineering*, vol. 10, no. 4, p. 523, 2020.
- [22] K. Vijayakumar, S. Senthilkumar, S. G. Chandratre, and V. Bharambe, "An analysis of arches of the foot: Grading the severity of pesplanus and pescavus using a newly designed podoscope and parameters," *Journal of The Anatomical Society of India*, vol. 70, no. 2, p. 85, 2021.
- [23] N. Laowattanatham, K. Chitsakul, S. Tretriluxana, and C. Hansasuta, "Smart digital podoscope for foot deformity assessment," in *The 7th 2014 Biomedical Engineering International Conference*, 2014: IEEE, pp. 1-5.
- [24] S. Chun, S. Kong, K.-R. Mun, and J. Kim, "A foot-arch parameter measurement system using a RGB-D camera," *Sensors*, vol. 17, no. 8, p. 1796, 2017.
- [25] J. A. Shrader, "Nonsurgical management of the foot and ankle affected by rheumatoid arthritis," *Journal of Orthopaedic & Sports Physical Therapy*, vol. 29, no. 12, pp. 703-717, 1999.
- [26] A. P. Ribeiro, I. C. Sacco, R. C. Dinato, and S. João, "Relationships between static foot alignment and dynamic plantar loads in runners with acute and chronic stages of plantar fasciitis: a cross-sectional study," *Brazilian Journal of Physical Therapy*, vol. 20, pp. 87-95, 2016.
- [27] P. R. Cavanagh and M. M. Rodgers, "The arch index: a useful measure from footprints," *Journal of biomechanics*, vol. 20, no. 5, pp. 547-551, 1987.
- [28] F. Hegazy, E. Aboelnasr, M. Abuzaid, I.-J. Kim, and Y. Salem, "Comparing Validity and Diagnostic Accuracy of Clarke's Angle and Foot Posture Index-6 to Determine Flexible Flatfoot in Adolescents: A Cross-Sectional Investigation," *Journal of Multidisciplinary Healthcare*, vol. 14, p. 2705, 2021.
- [29] K.-C. Chen, C.-J. Yeh, J.-F. Kuo, C.-L. Hsieh, S.-F. Yang, and C.-H. Wang, "Footprint analysis of flatfoot in preschool-aged children," *European journal of pediatrics*, vol. 170, no. 5, pp. 611-617, 2011.
- [30] J. C. Zuñil-Escobar, C. B. Martínez-Cepa, J. A. Martín-Urrialde, and A. Gómez-Conesa, "Medial longitudinal arch: accuracy, reliability, and correlation between navicular drop test and footprint parameters," *Journal of manipulative and physiological therapeutics*, vol. 41, no. 8, pp. 672-679, 2018.
- [31] L. T. Staheli, D. E. Chew, and M. Corbett, "The longitudinal arch. A survey of eight hundred and eighty-two feet in normal children and adults," *The Journal of bone and joint surgery. American volume*, vol. 69, no. 3, pp. 426-428, 1987.

- [32] T. Kasperczyk, "Wady postawy ciała", Kasper, Kraków, 2002.
- [33] K. Kaniewska, A. Kuryliszyn-Moskal, A. Hryniewicz, D. Moskal-Jasińska, M. Wojciuk, and Z. Dziecioł-Anikiej, "Static Foot Disturbances and the Quality of Life of Older Person with Rheumatoid Arthritis," *International journal of environmental research and public health*, vol. 19, no. 14, p. 8633, 2022.
- [34] T. Rutkowski, "Spine and Hip Range of Motion and Foot Morphology in Adolescent Female Ballet Dancers," *Sport i Turystyka Środkowoeuropejskie Czasopismo Naukowe*, vol. 4, no. 4, pp. 129-142, 2021.
- [35] S. F. Ameer, Z. T. Nayyef, Z. H. Fahad, and I. R. Niama ALRubea, "Using Morphological Operation and Watershed Techniques for Breast Cancer Detection," *International Journal of Online & Biomedical Engineering*, vol. 16, no. 5, 2020.
- [36] H. Miranda C, L. A. F. Cu, S. C. López, H. R. González, and M. C. Lara, "Interface for Contour Extraction and Determination of Morphologic Parameters in Digital Images of Footprints Based on Hernandez-Corvo Protocol," in *Latin American Conference on Biomedical Engineering*, 2019: Springer, pp. 367-376.